Int. J. Electrochem. Sci., 10 **(2015)** 4596 - 4603

International Journal of
ELECTROCHEMICAL
SCIENCE
www.electrochemsci.org

Preparation and Electrochemical Properties of $LiCu_xMn_{2-x}O_4$ ($x \leq 0.10$) Cathode Material by a Low-Temperature Molten-Salt Combustion Method

Jijun Huang[1,2], *Qiling Li*[1,2], *Hongli Bai*[1,2], *Wangqiong Xu*[1,2], *Yonghui He*[1,2], *Changwei Su*[1,2], *Jinhui Peng* [1,2], *Junming Guo*[1,2,*]

[1]Key Laboratory of Comprehensive Utilization of Mineral Resources in Ethnic Regions, Yunnan Minzu University, Kunming 650500, PR China
[2] Key Laboratory of Chemistry in Ethnic Medicinal Resources, State Ethnic Affairs Commission & Ministry of Education, School of Chemistry and Biotechnology, Yunnan Minzu University, Kunming 650500, PR China
[*]E-mail: guojunming@tsinghua.org.cn

Received: 24 February 2015 / *Accepted:* 12 April 2015 / *Published:* 28 April 2015

Single-phase $LiCu_xMn_{2-x}O_4$ cathode materials were prepared by a molten-salt combustion method. Surface morphology and particle size of the synthesized materials were characterized by scanning electron microscopy. With Cu doping, the average particle size decreased and distribution was more uniform. Galvanostatic charge-discharge experiments showed that Cu substitution in $LiMn_2O_4$ enhanced the cycling performance of the cathode material. $LiCu_{0.05}Mn_{1.95}O_4$ demonstrated excellent electrochemical performance with an initial discharge specific capacity of 119.0 mAh/g with 95.0% capacity retention after 100 cycles at 0.5 C (1 C = 148 mA/g). Rate performance, cyclic voltammetry, and electrochemical impedance spectroscopy tests show that Cu substitution improved the electrochemical properties of $LiMn_2O_4$.

Keywords: $LiMn_2O_4$, Cu-doping, molten-salt combustion method, lithium-ion battery

1. INTRODUCTION

The $LiMn_2O_4$ spinel compound has received a great deal of attention as the most promising positive electrode material for lithium-ion batteries because of its low cost, high safety, nontoxicity, and environmental friendliness [1-3]. However, capacity fading of $LiMn_2O_4$, mainly owing to structural distortion via the Jahn-Teller effect, is a fatal obstacle that limits its large-scale use. To suppress capacity fading, substitutions of the Mn^{3+} ions with other cations such as Mg^{2+} [4], Al^{3+} [5], and Ce^{4+} [6] have been studied. Results showed that ion doping is an effective way to improve the

structural stability and electrochemical performance of the $LiMn_2O_4$ cathode material. Cu doping affects the electrochemical properties of $LiMn_2O_4$ mainly because: 1) Cu doping can restrain the Jahn-Teller effect; and 2) the Cu-O bond energy is stronger than that of Mn-O, which can improve the structural stability.

In addition, the treatment process is an important factor in the electrochemical performance of spinel $LiMn_2O_4$ cathode material. $LiMn_2O_4$ has been prepared by solid-state [7], molten-salt [8], sol-gel [9], hydrothermal [10], and combustion methods [11]. The molten salt method generally uses carbonate or hydroxide as a raw material and excess KCl or LiOH as a molten medium or reactant. An advantage of this method is that the raw materials form a eutectic mixture that can promote the ion exchange rate. However, after preparation the samples must be washed with ethanol and distilled water to remove excess KCl or Li salts, which makes the process more complex. Combustion methods to produce ion-doped $LiMn_2O_4$ are attractive because of their rapid reaction rate, simplicity, and low cost. In addition, stoichiometric products can be obtained.

In this paper, $LiCu_xMn_{2-x}O_4$ cathode materials were prepared by a molten salt combustion synthesis. Low melting point lithium acetate (70 °C), manganese acetate (80 °C), and copper acetate (115 °C) were used as raw materials and fuel. This method does not require the addition of other fuel, and raw materials realize self-mixing during heating. In this work, the polarization, rate capability, and cycling performance of the $LiCu_xMn_{2-x}O_4$ cathode materials prepared by this method are investigated.

2. EXPERIMENTAL

2.1. Preparation of samples

The $LiCu_xMn_{2-x}O_4$ samples were prepared by a molten salt combustion synthesis method. First, stoichiometric amounts of lithium acetate, manganese acetate, and copper acetate were weighed and put into a 300-mL crucible. The mixture was heated in a muffle furnace at 400 °C for 1 h. The preheated powder was then ground and calcined at 600 °C for 3 h. The $LiCu_xMn_{2-x}O_4$ powders were obtained after cooling to room temperature.

2.2. Characterization

The crystalline structure of the $LiCu_xMn_{2-x}O_4$ samples was characterized by X-ray diffraction (D/max-TTRIII, Japan) with Cu Kα radiation in the 2θ angular range of 10-70° with 0.02° step size. Scan speed was 4° min^{-1}, with 30 mA operation current and 40 kV voltage. The morphology of the $LiCu_xMn_{2-x}O_4$ powders was observed by scanning electron microscopy (QUANTA-200; FEI Co., USA).

2.3. Electrochemical measurements

The cathodes were fabricated by dispersing 80 wt.% $LiCu_xMn_{2-x}O_4$ powders (active materials), 10 wt.% carbon black (conductive agent), and 10 wt.% polyvinylidene fluoride binder in N-methyl-2-

pyrrolidone solvent to form a homogeneous slurry, followed by plastering the slurry onto an aluminum foil current collector and drying at 120 °C overnight in a vacuum oven. All electrodes were cut into disks with a 16-mm diameter. For electrochemical measurements, CR-2025 coin-type cells were assembled in an argon-filled glove box using the above-prepared disks as cathode, metal lithium foil anode, polypropylene microporous film (Celgard 2320) separator, and 1.0 M $LiPF_6$ dissolved in a mixture of ethylene carbonate and dimethyl carbonate (1:1 by volume) as electrolyte. The galvanostatic charge and discharge tests of the cells were performed using a Land CT200 battery testing system (Wuhan Jinnuo Electronics Co., Ltd., China) at a current density of 0.5 C in the 3.0-4.5 V potential range. The cyclic voltammetry (CV) tests were conducted on an electrochemical workstation (IM6ex, ZAHNER-Elektrik GmbH & Co. KG, Germany) in the 3.5-4.6 V voltage range at a scanning rate of 0.05 mV s^{-1}. Electrochemical impedance spectroscopy (EIS) was carried out in the 0.1 Hz to 100 KHz frequency range with an AC signal amplitude of 10 mV using the IM6ex electrochemical workstation.

3. RESULTS AND DISCUSSION

3.1. Structure and morphology

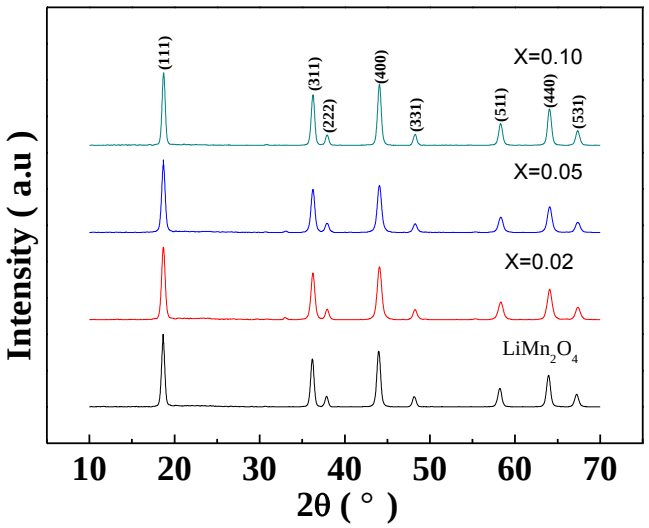

Figure 1. X-ray diffraction patterns of pristine $LiMn_2O_4$ and Cu-substituted $LiCu_xMn_{2-x}O_4$

In X-ray diffraction patterns of the $LiCu_xMn_{2-x}O_4$ obtained by the molten-salt combustion method (Fig. 1), all the materials prepared by the molten-salt combustion method show a single spinel phase, in good agreement with $LiMn_2O_4$ (JCPDS No. 35-0782). This indicates that the addition of Cu does not change the spinel structure of $LiMn_2O_4$. The scanning electron microscopy images of $LiCu_xMn_{2-x}O_4$ (x = 0, 0.02, 0.05, and 0.10) (Fig. 2) show that all the sample powders are agglomerations with a small grain size; the average particle is about 0.10-0.60 μm. As shown in Fig. 2,

the $LiMn_2O_4$ product agglomerated seriously, with non-uniform crystal size distribution. With Cu doping, the agglomeration decreased and the particle sizes decreased. The results indicate that Cu doping can restrain the agglomeration of the solid powders. The increased porosity of Cu-doped $LiMn_2O_4$ may increase the electrode-electrolyte contact area and facilitate lithium-ion transport, thus improving electrochemical performance.

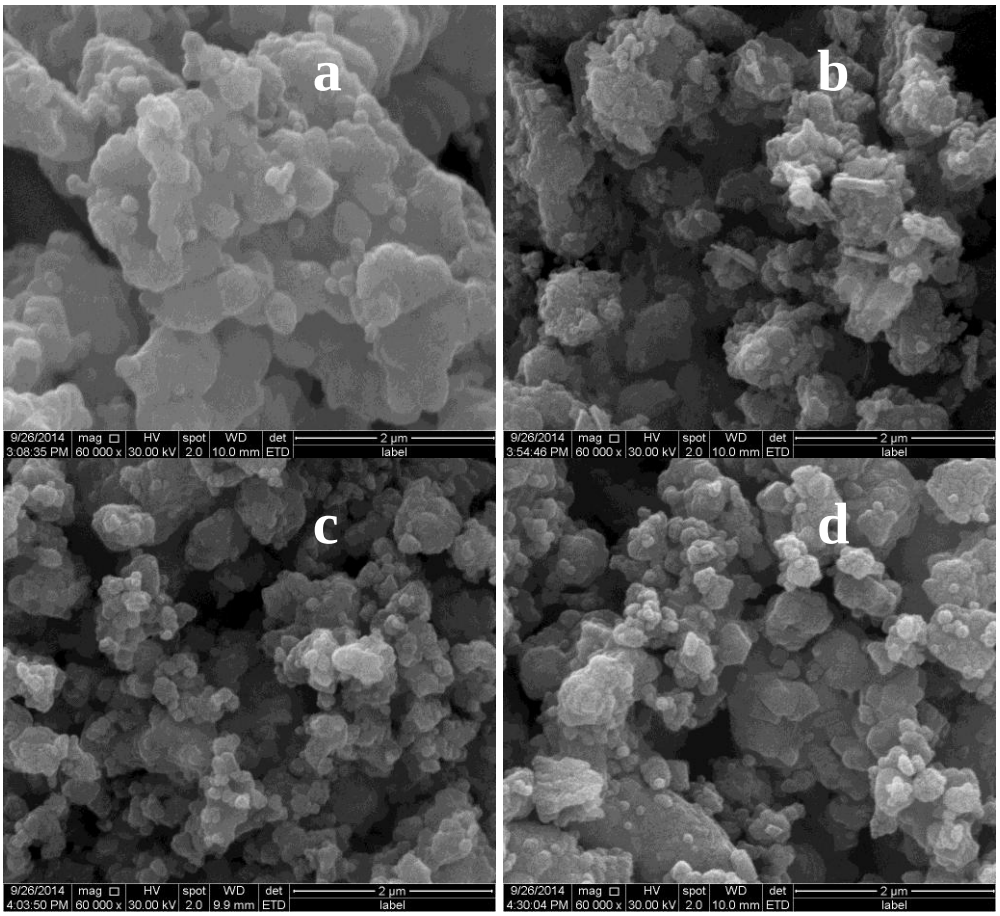

Figure 2. Scanning electron microscopy images of $LiCu_xMn_{2-x}O_4$ (a: x = 0, b: x = 0.02, c: x = 0.05, d: x = 0.10)

3.2 Galvanostatic charge/discharge studies

Figure 3(a) shows the first charge-discharge curves for $LiMn_2O_4$ and Cu-doped $LiCu_{0.05}Mn_{1.95}O_4$ cathode materials over the potential range of 3.0-4.5 V at 0.5 C charging rate. There are two plateaus for the first charge and discharge profiles for both samples: a plateau at 4.00 V corresponding to the $LiMn_2O_4/Li_{0.5}Mn_2O_4$ transformation, and a plateau at 4.15 V for the $Li_{0.5}Mn_2O_4/\lambda$-Mn_2O_4 transformation [12]. As seen in Fig. 3(b) and Table 1, the discharge-specific capacities of the $LiCu_xMn_{2-x}O_4$ products with x = 0, 0.02, 0.05, and 0.10 after 100 cycles were 91.1, 100.8, 113.1, and 91.9 mAh/g, respectively; and capacity retentions after 100 cycles were about 73.5%, 83.4%, 95.0%, and 88.4%. The discharge specific capacity and the capacity retention for

$LiCu_{0.05}Mn_{1.95}O_4$ after 100 charge cycles (113.1 mAh/g and 95.0%, respectively) were higher than those of the other samples.

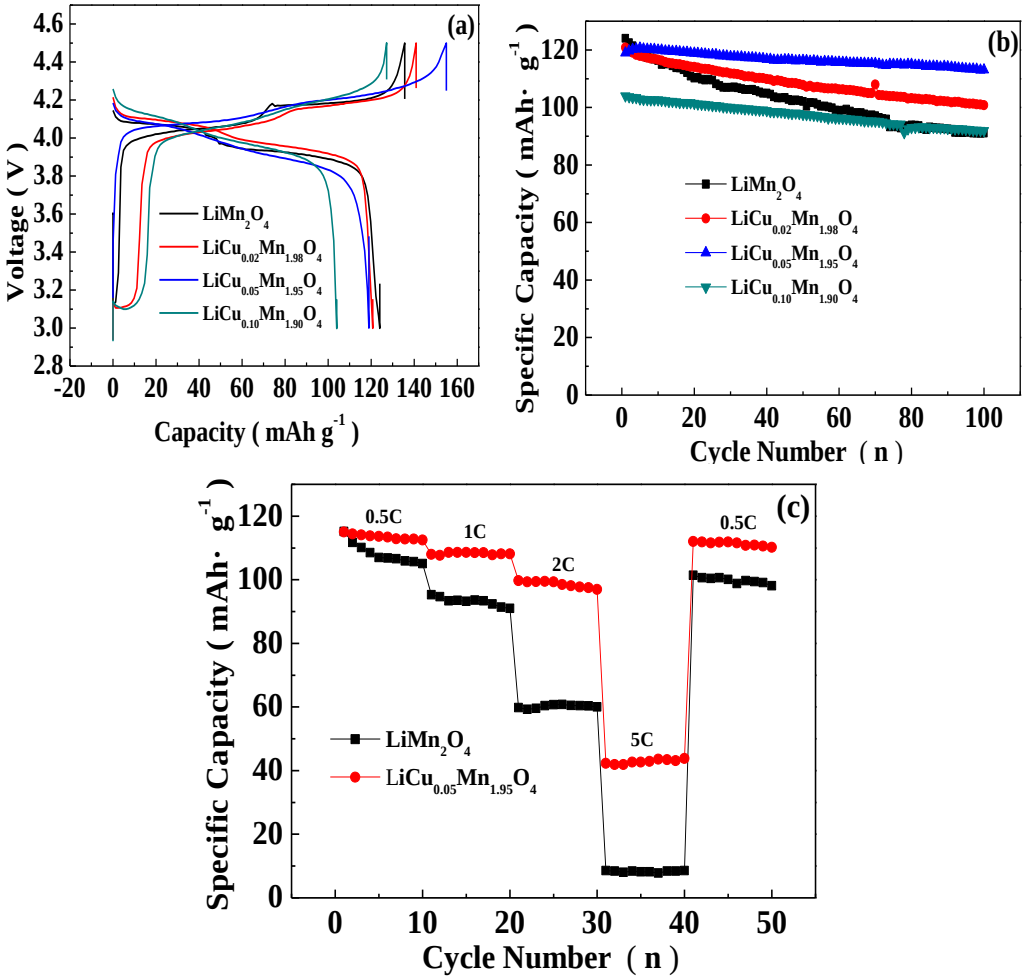

Figure 3. (a) First charge-discharge voltage profiles for $LiMn_2O_4$ and Cu-doped $LiCu_xMn_{2-x}O_4$; (b) Cycling performance at 0.5 C current rate; and (c) Discharge capacity vs. cycle number at various current rates from 0.5 C to 5 C (1 C = 148 mA/g) for $LiMn_2O_4$ and $LiCu_{0.05}Mn_{1.95}O_4$.

Therefore, the $LiCu_{0.05}Mn_{1.95}O_4$ product was optimal. Figure 3(c) shows the C-rate capabilities of the pristine $LiMn_2O_4$ and Cu-doped $LiCu_{0.05}Mn_{1.95}O_4$ cathode materials. For both compounds, the discharge capacity decreased as the C-rate increased, because of the low Li-ion diffusion rate in the $LiMn_2O_4$ particles. At 5 C, $LiCu_{0.05}Mn_{1.95}O_4$ delivered a discharge capacity of 42.3 mAh/g while the pristine $LiMn_2O_4$ sample hardly discharged. These results indicate that the Cu dose has a remarkable effect on the cycling behavior of $LiCu_{0.05}Mn_{1.95}O_4$. Cu doping affects the electrochemical properties of $LiMn_2O_4$ mainly as follows: 1) Cu doping can restrain the Jahn-Teller effect; and 2) the Cu-O bond strength is stronger than that of the Mn-O bond, which can improve the structural stability.

Table 1. Initial, 100th discharge capacities, and capacity retention of spinel $LiCu_xMn_{2-x}O_4$ (x = 0.0-0.10) cathode materials

Cathode materials	Discharge capacity (mAh/g)		capacity retention
	1st	100th	
$LiMn_2O_4$	124.0	91.1	73.5
$LiCu_{0.02}Mn_{1.98}O_4$	120.8	100.8	83.4
$LiCu_{0.05}Mn_{1.95}O_4$	119.0	113.1	95.0
$LiCu_{0.10}Mn_{1.90}O_4$	104.0	91.9	88.4

3.3. Cyclic voltammetric studies

Typical cyclic voltammograms of $LiMn_2O_4$ and Cu-substituted $LiCu_{0.05}Mn_{1.95}O_4$ electrodes in the potential range of 3.6-4.5 V at a scan rate of 0.05 mV s^{-1} are shown in Fig. 4. Li/$LiMn_2O_4$ and Li/$LiCu_{0.05}Mn_{1.95}O_4$ cells were tested before the galvanostatic charge-discharge studies at various current rates ranging from 0.5 C to 5 C. Both cells were again characterized by CV after the completion of 50 cycles at various current rates ranging from 0.5 C to 5 C. Figure 4 (a and b) shows CV curves for the initial and 50-cycled $LiMn_2O_4$ and $LiCu_{0.05}Mn_{1.95}O_4$. For the pristine $LiMn_2O_4$, in the first cycle, the two redox peaks are narrow and well separated. However, after the 50th cycle both the anodic and cathodic peaks are broader and closer to each other with weaker peak intensities compared with the first cycle; this is ascribed to possible Jahn-Teller distortions in the cycled samples. In contrast, after 50 cycles, $LiCu_{0.05}Mn_{1.95}O_4$ shows peaks similar to the pristine sample, indicating its smaller polarization and better reversibility [13]. Based on these results, Cu doping could significantly improve the reversibility and electrochemical performance of $LiMn_2O_4$.

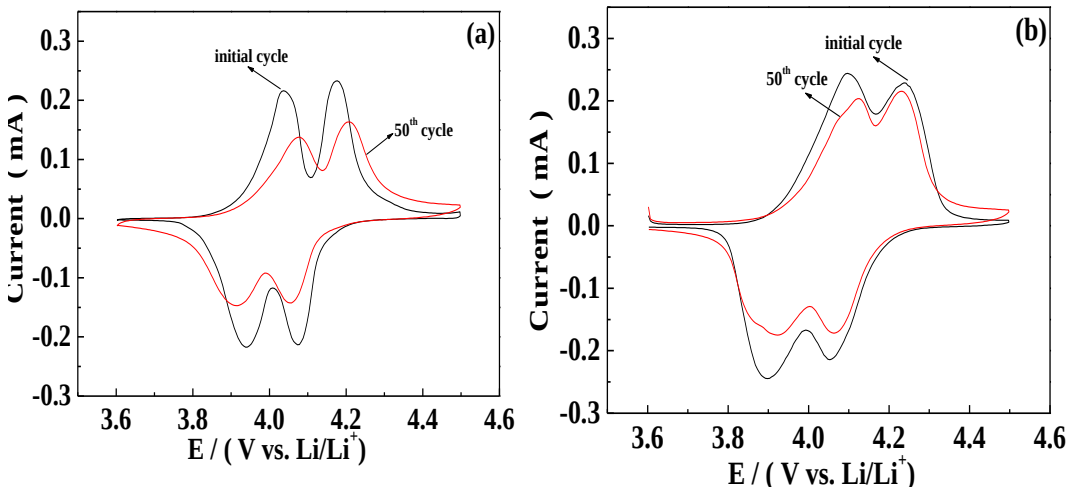

Figure 4. Typical CV curves of the initial and 50th cycles for (a) $LiMn_2O_4$ and (b) $LiCu_{0.05}Mn_{1.95}O_4$.

3.4 Electrochemical impedance spectroscopy

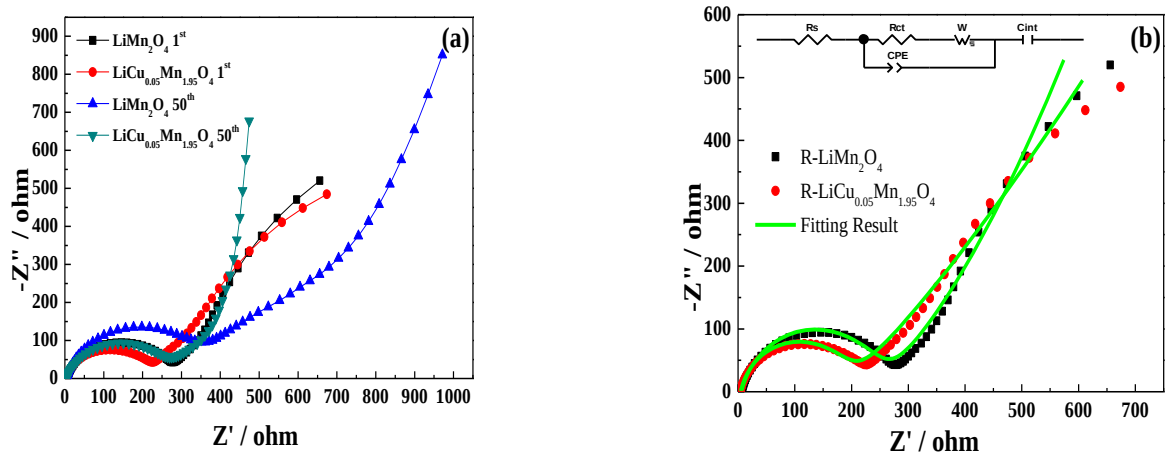

Figure 5. (a) Nyquist plots of pristine $LiMn_2O_4$ and Cu-doped $LiCu_{0.05}Mn_{1.95}O_4$ cathode materials at the 1st and 50th charge-discharge cycles, (b) Nyquist plots of pristine $LiMn_2O_4$ and Cu-doped $LiCu_{0.05}Mn_{1.95}O_4$ cathode materials at the 50th rate charge-discharge cycle. Insert is the equivalent circuit used to fit the EIS.

Table 2. Fitting values of electrochemical parameters obtained from EIS

Parameters	Cathode material	
	$LiMn_2O_4$	$LiCu_{0.05}Mn_{1.95}O_4$
R_s (Ω)	6.388	4.162
R_{ct} (Ω)	244.2	190.3

Nyquist plots for pristine $LiMn_2O_4$ and Cu-doped $LiCu_{0.05}Mn_{1.95}O_4$ cathode materials after 50 rate charge-discharge cycles are shown in Fig. 5 (a). The intercept at the real (Z') axis in high frequency corresponds to the solution resistance (Rs). The semicircle in the middle frequency range represents the charge-transfer resistance (Rct), which is the resistance of charge transfer between surface film and spinel particles. The inclined line corresponds to the Warburg impedance, which reflects the solid-state diffusion of Li-ions into $LiMn_2O_4$ particles, and the constant phase element represents the capacitance of a double layer [14]. It is evident that the charge transfer resistance (Rct) of $LiMn_2O_4$ increased to a large degree after 50 rate charge-discharge cycles, whereas the Rct of $LiCu_{0.05}Mn_{1.95}O_4$ increased by a small amount. This means that the charge transfer in $LiCu_{0.05}Mn_{1.95}O_4$ is easier, corresponding to its high rate capability and good cyclability as illustrated above. The EIS data can be analyzed by the equivalent circuit shown in the inset of Fig. 4b and the respective parameters in Table 3. The $LiCu_{0.05}Mn_{1.95}O_4$ sample has an Rct of 190.3 Ω, lower than that of the pristine sample (244.2 Ω). This indicates that Cu doping could effectively enhance the lithium-ion diffusibility in the spinel during the charge-discharge process. Hence, this result suggests that Cu-doped $LiCu_{0.05}Mn_{1.95}O_4$ is favorable for high-rate performance, as shown in Fig. 3.

4. CONCLUSIONS

Single-phase $LiCu_xMn_{2-x}O_4$ spinels were synthesized by a low-temperature molten-salt combustion method. The agglomeration of the sample and particle sizes decreased with Cu doping. $LiCu_{0.05}Mn_{1.95}O_4$, with 95.0% capacity retention at 0.5 C (1C = 148mA/g) discharge rate after 100 cycles, shows excellent cycling stability. Rate performance, CV, and EIS tests show that Cu-substituted spinels have a high rate capability and reversible cycling performance.

ACKNOWLEDGEMENTS
This work was financially supported by the National Natural Science Foundation of China (51262031, 51462036), Program for Innovative Research Team (in Science and Technology) in University of Yunnan Province (2011UY09), Yunnan Provincial Innovation Team (2011HC008), the Natural Science Foundation of Yunnan Provincial Education Department (2014J079), and Innovation Program of Yunnan Minzu University (2013HXSRTY01, 2014YJZ10, 2014YJY74).

References

1. J. Yao, L. Lv, C. Shen, P. Zhang, K. Francois, A. Zinsou and L. Wang, *Ceram. Int.*, 39 (2013) 3359-3364.
2. T. Yi, L. Yin, Y. Ma, H. Shen, Y. Zhu and R. Zhu, *Ceram. Int.*, 39 (2013) 4673-4678.
3. B. Ebin, S. Gürmen and G. Lindbergh, *Ceram. Int*., 40 (2014) 1019-1027.
4. M. W. Xiang, C.W. Su, L. L. Feng, M. L. Yuan and J. M. Guo, *Electrochim. Acta.*, 125 (2014) 524-529.
5. L. Xiao, Y. Zhao, Y. Yang, Y. Cao, X. Ai and H. Yang, *Electrochim. Acta.*, 54 (2008) 545-550.
6. D. Arumugam, G.P. Kalaignan, *J. Electroanal. Chem.*, 648 (2010) 54-59.
7. Y. Cai, Y. Huang, X. Wang, D. Jia and X. Tang, *Ceram. Int.*, 40 (2014) 14039-14043.
8. M. Helan, L.J. Berchmans, T.P. Jose, A. Visuvasam and S. Angappan, *Mater Chem Phy.*, 124 (2010) 439-442.
9. F. X. Wang, S. Y. Xiao, Y. Shi, L. L. Liu, Y. S. Zhu, Y. P. Wu, J. Z. Wang and R. Holze, *Electrochim. Acta.*, 93 (2013) 301-306.
10. X. Lv, S. Chen, C. Chen, L. Liu, F. Liu and G. Qiu, *Solid State Sciences.*, 31 (2014) 16-23.
11. W. Yang, G. Zhang, J. Xie, L. Yang and Q. Liu, *J. Power Sources.*, 81–82 (1999) 412–415.
12. H. Yim, W. Y. Kong, S. J. Yoon, S. Nahm, H. W. Jang, Y. E. Sung, J. Y. Ha, A. V. Davydov and J. W. Choi, *Electrochem. Comm.*, 43 (2014) 36–39.
13. D. Arumugam, G. P. Kalaignan, K. Vediappan and C.W. Lee, *Electrochim. Acta.*, 55 (2010) 8439-8444.
14. X. Zhang, Y. Xu, H. Zhang, C. Zhao and X. Qian, *Electrochim. Acta.*, 145 (2014) 201-208.